Journal of Superconductivity and Novel Magnetism
https://doi.org/10.1007/s10948-017-4517-3

ORIGINAL PAPER

Spin Transfer Torque Switching in Pentalayer Nanopillar with Biquadratic Coupling

D. Aravinthan[1] · P. Sabareesan[2] · M. Daniel[3]

Received: 17 November 2017 / Accepted: 5 December 2017

Abstract
The effect of biquadratic coupling on spin transfer torque-assisted magnetization switching in the pentalayer nanopillar device is studied by numerically solving the magnetization switching dynamics of the free layer governed by the Landau-Lifshitz-Gilbert-Slonczewski (LLGS) equation. Magnetization switching time in the absence of biquadratic coupling for an applied current density of $10 \times 10^{11} \mathrm{Am}^{-2}$ is 186 ps. Biquadratic coupling arises due to the uncorrelated roughness in the ferromagnetic layers and it reduces the switching time to 160 ps. Further, the impact of the period of roughness and spacer layer thickness on switching time are studied.

Keywords Ultrafast magnetization dynamics · Multilayer · Magnetization switching · Spin transfer torque · Nanopillar · Switching time

1 Introduction

Ultrafast magnetization switching assisted by a spin transfer torque has been received a considerable interest in recent years, due to its potential applications in future spintronic devices such as magnetic random access memories [1, 2] and high frequency microwave oscillators [3, 4]. The basic structure used in the memory devices is a trilayer structure which consists of two ferromagnetic layers and a non-magnetic spacer layer. Magnetization of the first ferromagnetic layer is fixed, and hence, it acts as a polarizer, when current passed through it. Spin polarized electrons reaches the second ferromagnetic layer (free layer) and that produces a spin torque due to the exchange interaction between local magnetization and spin angular momentum [5]. This spin torque will switch the magnetization of the free layer, when the applied current is above the critical value [6]. The reduction of the critical current density and the switching time are the two important issues to develop potential applications. Fuchs et al. [7] introduced a pentalayer structure based on the proposal from Berger [8], in order to reduce the critical current density and the switching time by increasing the spin transfer torque efficiency. In the pentalayer structure, additional spacer layer and a ferromagnetic pinned layer are added above the trilayer structure and showed that spin torque efficiency is increased, when the pinned layers are anti-aligned [9]. The enhanced spin transfer torque increases the switching speed and reduces the switching time and critical current density required to initiate the magnetization switching [10, 11]. Since then, the spin transfer torque magnetization switching in pentalayer nanopillar has been widely studied both theoretically [12–15] and experimentally [16, 17]. Growing a pentalayer nanopillar for magnetization switching applications in a smooth fashion without roughness is very difficult. Hence, the resultant pentalayer structure have a certain interface roughness, and they give rise to two different coupling mechanisms [18]. First one is biquadratic coupling which arises due to the uncorrelated interface roughness [19] and the second

✉ P. Sabareesan
sendtosabari@gmail.com

D. Aravinthan
d.aravinthan@gmail.com

M. Daniel
danielcnld@gmail.com

[1] Centre for Nonlinear Dynamics, School of Physics, Bharathidasan University, Tiruchirappalli, 620024 Tamilnadu, India

[2] Centre for Nonlinear Science and Engineering, School of Electrical and Electronics Engineering, SASTRA University, Thanjavur, 613401 Tamilnadu, India

[3] SNS Institutions, Coimbatore, 641049 Tamilnadu, India

Published online: 15 December 2017

one is orange peel coupling (Néel coupling) which arises due to the correlated interface roughness [20]. We have recently studied the effect of both orange peel coupling [21] and biquadratic coupling [22] on current induced magnetization switching in trilayer nanopillar structure. In this paper, we study the effect of biquadratic coupling on spin torque magnetization switching in a pentalayer nanopillar device. Biquadratic coupling was first phenomenologically introduced by Rührig et al. in 1991 [23]. The energy expression describing two coupled magnetic layers of the form $\frac{E}{A} = -J_2(\mathbf{m}_1 \cdot \mathbf{m}_2)^2$, is called as biquadratic, because it is quadratic in both of the magnetization directions [18], where E and A are the energy and unit surface area of the interface, respectively. $\mathbf{m}_1$ and $\mathbf{m}_2$ are unit magnetization vectors of the first and second magnetic layers, respectively. J_2 is the coupling strength. All measured values of J_2 are negative, favoring perpendicular orientations of the magnetization. Biquadratic coupling can be experimentally studied by measuring the field dependence of the direction and value of the macroscopic magnetic moment of the sample using the techniques such as Magneto-optical Kerr effect (MOKE), magnetometry, vibrating sample magnetometry (VSM), superconducting quantum interface device (SQUID) magnetometry, alternating gradient magnetometry (AGM) [24]. The first hint for the existence of the biquadratic in Fe/Cr/Fe trilayer was observed independently by Grünberg et al. [25] and Unguris et al. [26] in 1991. Existence of biquadratic was firmly established by Rührig et al. [23] and it has been investigated in detail by several other groups [27–34]. Although biquadratic was studied for many systems, there is no general theory for biquadratic coupling which can be adopted for all systems. Biquadratic coupling arises due to anyone of the following origin: intrinsic origin (angular dependence of exchange energy) [35–39], extrinsic thickness fluctuations [40, 41], indirect exchange through unpaired spin ("loose spin" model) [42], and uncorrelated roughness interface [19, 43]. We investigate the effect of biquadratic coupling occurs due to the magnetic dipole field created by a uncorrelated roughness of the free and pinned layers. This can be done by solving the magnetization switching dynamics of the free layer governed by the Landau-Lifshitz-Gilbert-Slonczewski (LLGS) equation. The structure of the paper is organized as follows. Sketch of the pentalayer nanopillar taken for our study and the construction of the dynamical equation (LLGS) expressing the magnetization switching dynamics of the free layer are described in Section 2. Numerical integration of the LLGS equation and the results are discussed in Section 3. Concluding remarks are made in Section 4.

2 Model and Dynamical Equation

The pentalayer nanopillar structure consisting of three ferromagnetic layers (two pinned layer and one free layer) and two non-magnetic metal (spacer) layers is taken for our study and the schematic diagram of the pentalayer nanopillar is given in Fig. 1. The magnetization of the first pinned layer (bottom) having large thickness is pinned along the easy axis of the magnetization. The thickness of the second pinned layer (top) is smaller than that of the first one and its magnetization is pinned opposite to the first one, in order to increase the spin transfer efficiency. Both pinned layers have periodic interfacial roughness with a period L and a height δ. Thickness of the free layer is thinner than the second pinned layer, and its magnetization is free to move and it have in-plane anisotropy. Two thinner non-magnetic metal spacers are kept in between the ferromagnetic layers

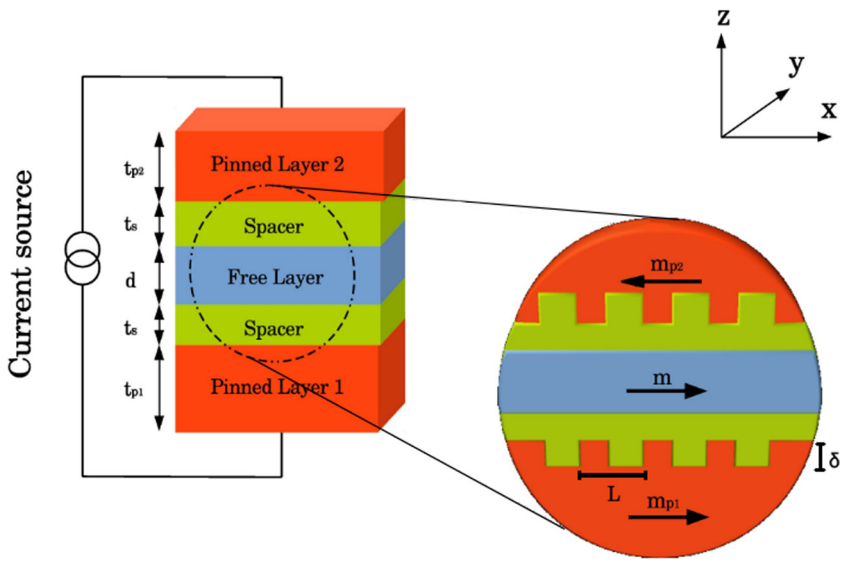

Fig. 1 A sketch of the pentalayer nanopillar with biquadratic coupling. In the zoomed view, we see the pinned layers have the periodic interfacial terraces with a period L and a height δ. $\mathbf{m}$, $\mathbf{m}_{p1}$ and $\mathbf{m}_{p2}$ represent the magnetization of the free layer, first pinned layer and second pinned layer respectively

to avoid the direct coupling between the ferromagnetic layers. Current is supplied normal to the plane of the device (z-direction) and it becomes spin polarized, when it passes through the pinned layer. The polarized current entered into the interface of the free layer produces a spin transfer torque (STT) due to the exchange coupling between the spins of the conduction electron and local magnetization, and it switches the magnetization of the free layer. The electrons scattered from the free layer reaches the second pinned layer. Since the magnetization of the second pinned layer is aligned anti-parallel to the free layer (high resistance configuration), the electrons are reflected back into the free layer. The reflected electrons produces an additional STT in the free layer, which reduces the critical current density and the switching time. The magnetization switching dynamics of the free layer in the pentalayer is governed by the LLGS equation and it can be written in dimensionless form as [44],

$$\frac{d\mathbf{m}}{d\tau} = -[\mathbf{m}\times\mathbf{h_{eff}}] - \alpha[\mathbf{m}\times(\mathbf{m}\times\mathbf{h_{eff}})] + a_{j1}[\mathbf{m}\times(\mathbf{m}\times\mathbf{m}_{p1})] - a_{j2}[\mathbf{m}\times(\mathbf{m}\times\mathbf{m}_{p2})] \quad (1a)$$

$$\mathbf{m} = (m^x, m^y, m^z), \quad \mathbf{m}^2 = m^{x2} + m^{y2} + m^{z2} = 1 \quad (1b)$$

where $\mathbf{m} = \frac{\mathbf{M}}{M_s}$ is the dimensionless magnetization of the free layer, $\tau = \gamma M_s t$ is the dimensionless time variable. Here, γ is gyromagnetic ratio, M_s is saturation magnetization of the free layer. α is the Gilbert damping parameter, $a_{j1} = a_{j2} = a_j = \frac{pJ\hbar}{\mu_0 e d M_s^2}$ is the spin transfer torque coefficient, and its value is positive when electrons flow from pinned layer to free layer (i.e., thicker layer to thinner layer) and negative when electrons transfer from free layer to pinned layer (i.e., thinner to thicker layer) [6]. Here, p is the polarization factor, J is the current density applied, $\hbar$ is reduced Planck's constant, μ_0 is the permeability of the free space, e is the electron's charge, d is the thickness of the free layer. $\mathbf{m_{p1}}$ and $\mathbf{m_{p2}}$ are the unit magnetization vectors in first and second pinned layer, respectively. The effective magnetic field $\mathbf{h}_{eff}$ due to various magnetic anisotropic contributions and due to external field acting on the free layer can be written as,

$$\mathbf{h}_{eff} = (h_a + h_b)m^x\mathbf{e}^x + h_e\mathbf{e}^y - N_z m^z\mathbf{e}^z. \quad (2)$$

Magnetization of the free layer taken for our study is aligned along its easy axis (x-axis) and hence, magneto-crystalline anisotropy acts along x-axis. h_a is the field term due to magneto-crystalline anisotropy and $\mathbf{e}^x$ is the unit vector along x-axis. h_b is biquadratic coupling field arises due to the uncompensated magnetic poles present in the edges of the both pinned layers and its value can be written as [19, 45],

$$h_b = \frac{\mu_0 M_s^2 \delta^2 L}{2\pi^3 A_{ex} d} \exp\left(\frac{-4\pi t_s}{L}\right)\left[1 - \exp\left(\frac{-8\pi d}{L}\right)\right]. \quad (3)$$

Here, A_{ex} is the exchange stiffness constant of the free layer, d is the thickness of the free layer and t_s is the thickness of the spacer layer, δ and L are height and period of the roughness of the pinned layer, respectively. In (2), h_e represents the external magnetic field applied perpendicular to the easy axis (along y-direction) and $\mathbf{e}^y$ is the unit vector along y-axis. N_z represents the demagnetization factor along z-direction, which arises due to the shape anisotropy present in the system and $\mathbf{e}^z$ is the unit vector along z-axis. By substituting the total effective magnetic field found in (2) into (2), and write the LLGS equation in component form as,

$$\frac{dm^x}{d\tau} = (h_e + N_z m^y)m^z - \alpha[h_e m^x m^y - (h_a + h_b + N_z)m^x m^{z^2} - (h_a + h_b)m^x m^{y^2}] - a_{j1}(m^{y^2} + m^{z^2}) - a_{j2}(m^{y^2} + m^{z^2}) \quad (4a)$$

$$\frac{dm^y}{d\tau} = -(h_a + h_b + N_z)m^x m^z + \alpha[(h_e - (h_a + h_b)m^y)m^{x^2} + (h_e + N_z m^y)m^{z^2}] + a_{j1}m^x m^y + a_{j2}m^x m^y \quad (4b)$$

$$\frac{dm^z}{d\tau} = (h_a + h_b)m^x m^y - h_e m^x - \alpha[(h_a + h_b + N_z)m^{x^2} m^z + (h_e + N_z m^y)m^y m^z] + a_{j1}m^x m^z + a_{j2}m^x m^z. \quad (4c)$$

Equations (4a)–(4c) are the first order dimensionless LLGS equations by solving the set of above three equations, magnetization switching dynamics of the free layer can be studied and it is discussed in the next section.

3 Magnetization Switching Macrospin Dynamics: A Numerical Study

The set of three first order dimensionless LLGS equations (4a)–(4c) are numerically integrated using Runge-Kutta fourth order procedure and various parameters used for the numerical simulation are given in Table 1. After solving the dimensionless LLGS equations, the dimensionless time variable τ is converted into dimension time variable t by using the transformation $t = \tau/\gamma M_s$. In order to suppress the ringing effect and oscillations in the magnetization switching, we have chosen the value of applied current density and Gilbert damping factor as, $J = 10 \times 10^{11} Am^{-2}$ and $\alpha = 0.001$, respectively. First, the impact of biquadratic coupling on switching time is studied by solving the LLGS equation both in the absence and in the presence of biquadratic coupling. Then, impact of period of roughness and spacer layer thickness on switching time are studied by varying their respective parameter. The numerical results of each study is presented in the forthcoming sections.

Table 1 Values of various parameters used in the calculations [21, 22]

Parameter	Symbol	Value
Polarization factor	p	0.3
Gilbert damping parameter	α	0.001
Magneto-crystalline anisotropy field of the free layer	h_a	0.01
Saturation magnetization of the free layer	M_s	$0.795 \times 10^6 Am^{-1}$
Exchange stiffness constant of the free layer	A_{ex}	$2.1 \times 10^{-11} Jm^{-1}$
Thickness of the free layer	d	$2.8 \times 10^{-9} m$
Thickness of spacer layer	t_s	$2 \times 10^{-9} m$
Height of the roughness of the pinned layer	δ	$0.8 \times 10^{-9} m$
Period of the roughness of the pinned layer	L	$40 \times 10^{-9} m$

3.1 Impact of Biquadratic Coupling on the Switching Time

First, the set of three first order LLGS (4a)–(4c) are numerically solved in the absence and in the presence of biquadratic coupling separately and the results obtained are plotted in Fig. 2. The magnetization (**m**) of the free layer is initially aligned along the positive x-direction ($m^x = 1$). The current passing through the pinned layer becomes spin polarized and the polarized electrons enter into the free layer produces a spin transfer torque. As a response to the spin transfer torque and damping torque, the free layer magnetization undergoes an elliptical precession and reaches the switched state ($m^x = -1$). The time taken for switching the magnetization from $m^x = +1$ to $m^x = -1$ is called the switching time and its value in the absence of biquadratic coupling is 186 ps for an applied current density of $10 \times 10^{11} Am^{-2}$. The presence of biquadratic coupling reduces the switching time to 160 ps (shown in Fig. 2). The reason for reduction of switching time in the presence of biquadratic coupling is understood from the magnetization trajectory in m^y - m^z plane as shown in Fig. 3.

In the absence of biquadratic coupling, the free layer magnetization reaches the hard axis $m^y = +1$ near $m^z = -0.45$ as a response to spin transfer torque. However, when there exists a biquadratic coupling, the free layer magnetization reaches the hard axis $m^y = +1$ near $m^z = -0.20$ itself, i.e., the spiraling path of the free layer magnetization in the m^y - m^z plane in the presence of biquadratic coupling is very short compared to that of the same in the absence of biquadratic coupling. Additional biquadratic coupling field that arises due to the uncompensated magnetic poles presented in the edges of the pinned layers, moves the magnetization of the free layer from the easy axis to another stable state very fast and hence the presence of biquadratic coupling reduces the switching time. Therefore, the fastest magnetization switching in pentalayer structure can be achieved in the presence of biquadratic coupling and it is in good agreement with the results obtained for the trilayer structure [22]. Since, biquadratic coupling arises due to the roughness in the pinned layer, we study the impact of the period of

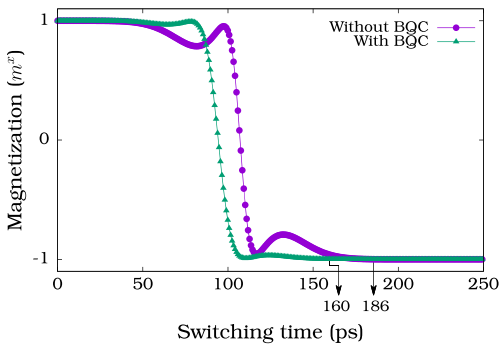

Fig. 2 A plot of the free layer magnetization versus switching time for the pentalayer nanopillar in the presence and in the absence of the biquadratic coupling (BQC) for an applied current density of $J = 10 \times 10^{11} Am^{-2}$. The presence of biquadratic coupling reduces the switching time from 186 ps to 160 ps

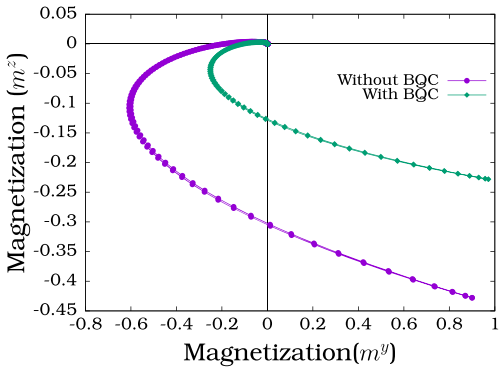

Fig. 3 Magnetization trajectory in m^y - m^z plane for the presence and for the absence of biquadratic coupling (BQC)

roughness on the switching time and the results of the same are presented in the next section.

3.2 Impact of Period of Roughness on the Switching Time

In order to understand the effect of the period of roughness on the switching time, the first order LLGS (4a)–(4c) are numerically integrated by varying the period of roughness (L) from 0 to 100 nm. The data obtained from the numerical simulation for an applied current density of $10 \times 10^{11} Am^{-2}$ are plotted in Fig. 4. The switching time in the absence of biquadratic coupling is found to be 186 ps and when the period of roughness is increased, the switching time of the free layer magnetization decreases, and it saturates near 100 nm. When the period of roughness increases, the uncompensated magnetic poles presented in the edges of the pinned layers increases and it increases the biquadratic coupling field acting on the free layer which reduces the switching time. When the period of roughness of our device is set as 40 nm, the switching time is found as 160 ps, which is perfectly matches with the result in Fig. 2. In order to understand the effect of spacer layer thickness on biquadratic coupling field, we study the impact of spacer layer thickness on the switching time and their numerical results are presented in the next section.

3.3 Impact of Spacer Layer Thickness on the Switching Time

Effect of spacer layer thickness on the switching time is studied by numerically simulating the first order LLGS equations given in (4a)–(4c), by varying the spacer layer thickness from 1 nm to 10 nm. The data obtained for an applied current density of $10 \times 10^{11} Am^{-2}$ is plotted in Fig. 5. It is found that the switching time increases from 155 ps to 182 ps, when the thickness of the spacer layer

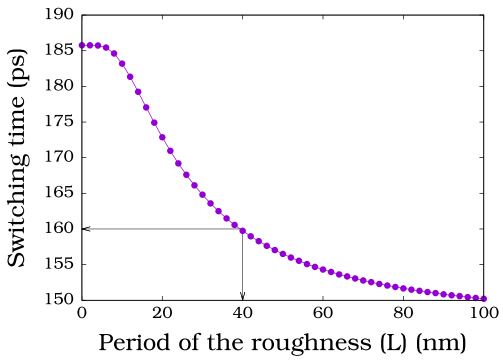

Fig. 4 A plot of period of the roughness versus switching time for the pentalayer nanopillar for an applied current density of $J = 10 \times 10^{11} Am^{-2}$. The switching time decreases when the period of the roughness is decreased

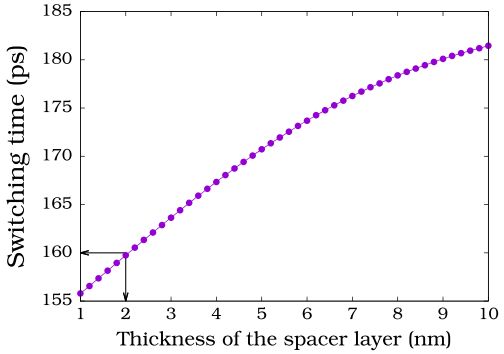

Fig. 5 A plot of thickness of the spacer layer versus switching time for an applied current density of $J = 10 \times 10^{11} Am^{-2}$. The switching time increases when the thickness of the spacer layer is increased

is increased from 1 to 10 nm as found in Fig. 5. The biquadratic coupling field acting on the free layer decreases exponentially, when the thickness of the spacer layer is increased, and hence the switching time increases. When the thickness is beyond 10 nm, the effect due to biquadratic coupling is negligible and the switching occurs only due to the spin transfer torque. When the thickness of the spacer layer of our device is 2 nm, the switching time is found as 160 ps, and it exactly matches with the result in Fig. 2.

4 Conclusions

The spin transfer torque assisted magnetization switching in the pentalayer nanopillar with biquadratic coupling is studied by numerically solving the LLGS equation. The presence of biquadratic coupling reduces the switching time from 186 to 160 ps for an applied current density of $10 \times 10^{11} Am^{-2}$. Reduction of switching time in the presence of biquadratic coupling is also confirmed by the magnetization trajectory in m^y-m^z plane. Further, the effect of period of roughness and spacer layer thickness on switching time is also studied. Switching time of the free layer in the pentalayer nanopillar device can be reduced by fabricating the pentalayer nanopillar with biquadratic coupling and with minimal thickness.

Acknowledgments D. A acknowledges Department of Science and Technology (DST) for the award of DST-INSPIRE Fellowship. P. S acknowledges DST for the award of SERB - Young Scientist project (SB/FTP/PS-061/2013).

References

1. Chappert, C., Fert, A., Van Dau, F.N.: Nat. Mater. **6**(11), 813 (2007)
2. Katine, J.A., Fullerton, E.E.: J. Magn. Magn. Mater. **320**, 1217 (2008)

3. Kaka, S., Pufall, M.R., Rippard, W.H., Silva, T.J., Russek, S.E., Katine, J.A.: Nature **437**(7057), 389 (2005)
4. Carpentieri, M., Lattarulo, F.: IEEE Trans. Magn. **49**, 3151 (2013)
5. Slonczewski, J.C.: J. Magn. Magn. Mater. **159**(1), L1 (1996)
6. Li, Z., Zhang, S.: Phys. Rev. B **68**(2), 024404 (2003)
7. Fuchs, G.D., Krivorotov, I.N., Braganca, P.M., Emley, N.C., Garcia, A.G.F., Ralph, D.C., Buhrman, R.A.: Appl. Phys. Lett. **86**, 152509 (2005)
8. Berger, L.: J. Appl. Phys. **93**(10), 7693 (2003)
9. Meng, H., Wang, J., Wang, J.P.: Appl. Phys. Lett. **88**, 082504 (2006)
10. Huai, Y., Pakala, M., Diao, Z., Ding, Y.: Appl. Phys. Lett. **87**, 222510 (2005)
11. Wang, R.X., He, P.B., Li, Z.D., Pan, A.L., Liu, Q.H.: J. Appl. Phys. **109**, 033905 (2011)
12. Apalkov, D., Pakala, M., Huai, Y.: J. Appl. Phys. **99**(8), 08B907 (2006)
13. Finocchio, G., Azzerboni, B., Fuchs, G.D., Buhrman, R.A., Torres, L.: J. Appl. Phys. **101**(6), 063914 (2007)
14. Mojumder, N.N., Augustine, C., Nikonov, D.E., Roy, K.: J. Appl. Phys. **108**(10), 104306 (2010)
15. Makarov, A., Sverdlov, V., Osintsev, D., Selberherr, S.: Phys. Status Solidi RRL **5**, 420 (2011)
16. Diao, Z., Panchula, A., Ding, Y., Pakala, M., Wang, S., Li, Z., Apalkov, D., Nagai, H., Driskill-Smith, A., Wang, L.C., Chen, E., Huai, Y.: Appl. Phys. Lett. **90**(13), 132508 (2007)
17. Chun, B.S., Fowley, C., Abid, M., Coey, J.M.D.: J. Phys. D: Appl. Phys. **43**(2), 025002 (2010)
18. Stiles, M.D.: Ultrathin Magnetic Structures III. In: Bland, J., Heinrich, B. (eds.), pp. 99–142. Springer, Berlin (2005)
19. Demokritov, S., Tsymbal, E., Grünberg, P., Zinn, W., Schuller, I.K.: Phys. Rev. B **49**, 720 (1994)
20. Néel, L.: C. R. Acad. Sci. **255**, 1676 (1962)
21. Aravinthan, D., Sabareesan, P., Daniel, M.: AIP Advan. **5**(7), 077166 (2015)
22. Aravinthan, D., Sabareesan, P., Daniel, M.: AIP Conf. Proc. **1731**(1), 130032 (2016)
23. Rührig, M., Schäfer, R., Hubert, A., Mosler, R., Wolf, J.A., Demokritov, S., Grünberg, P.: Phys. Status Solidi (a) **125**(2), 635 (1991)
24. Demokritov, S.O.: J. Phys. D: Appl. Phys. **31**(8), 925 (1998)
25. Grünberg, P., Demokritov, S., Fuss, A., Vohl, M., Wolf, J.A.: J. Appl. Phys. **69**(8), 4789 (1991)
26. Unguris, J., Celotta, R.J., Pierce, D.T.: Phys. Rev. Lett. **67**, 140 (1991)
27. Pierce, D.T., Unguris, J., Celotta, R.J.: Ultrathin Magnetic Structures II. In: Bland, J.A.C., Heinrich, B. (eds.), pp. 117–147. Springer, Berlin (2005)
28. Fullerton, E.E., Riggs, K.T., Sowers, C.H., Bader, S.D., Berger, A.: Phys. Rev. Lett. **75**, 330 (1995)
29. Elmers, H.J., Liu, G., Fritzsche, H., Gradmann, U.: Phys. Rev. B **52**, R696 (1995)
30. Meersschaut, J., Dekoster, J., Schad, R., Beliën, P., Rots, M.: Phys. Rev. Lett. **75**, 1638 (1995)
31. Schreyer, A., Ankner, J.F., Zeidler, T., Zabel, H., Majkrzak, C.F., Scháfer, M., Grúnberg, P.: Europhys. Lett. **32**(7), 595 (1995)
32. Grimsditch, M., Kumar, S., Fullerton, E.E.: Phys. Rev. B **54**, 3385 (1996)
33. Hicken, R., Daboo, C., Gester, M., Ives, A., Gray, S., Bland, J.A.C.: Thin Solid Films **275**(1), 199 (1996)
34. Azevedo, A., Chesman, C., Rezende, S.M., de Aguiar, F.M., Bian, X., Parkin, S.S.P.: Phys. Rev. Lett. **76**, 4837 (1996)
35. Erickson, R.P., Hathaway, K.B., Cullen, J.R.: Phys. Rev. B **47**, 2626 (1993)
36. Edwards, D., Ward, J., Mathon, J.: J. Magn. Magn. Mater. **126**(1), 380 (1993)
37. Barnaš, J., Grünberg, P.: J. Magn. Magn. Mater. **121**(1), 326 (1993)
38. Inoue, J.: J. Magn. Magn. Mater. **136**(3), 233 (1994)
39. Spišák, D., Hafner, J.: J. Magn. Magn. Mater. **168**(3), 257 (1997)
40. Slonczewski, J.C.: Phys. Rev. Lett. **67**, 3172 (1991)
41. Slonczewski, J.: J. Magn. Magn. Mater. **150**(1), 13 (1995)
42. Slonczewski, J.C.: J. Appl. Phys. **73**(10), 5957 (1993)
43. Rücker, U., Demokritov, S., Tsymbal, E., Grünberg, P., Zinn, W.: J. Appl. Phys. **78**(1), 387 (1995)
44. Aravinthan, D., Sabareesan, P., Daniel, M.: J. Magn. Magn. Mater. **421**, 409 (2017)
45. Rijks, T.G.S.M., Reneerkens, R.F.O., Coehoorn, R., Kools, J.C.S., Gillies, M.F., Chapman, J.N., de Jonge, W.J.M.: J. Appl. Phys. **82**(7), 3442 (1997)